Title

Hyporheic Zone Microbiome Assembly Is Linked to Dynamic Water Mixing Patterns in Snowmelt-Dominated Headwater Catchments

Journal

Journal of Geophysical Research Biogeosciences, 124(11)

ISSN

2169-8953

Authors

Saup, CM
Bryant, SR
Nelson, AR
et al.

Publication Date

2019-11-01

DOI

10.1029/2019jg005189

Peer reviewed

Hyporheic Zone Microbiome Assembly Is Linked to Dynamic Water Mixing Patterns in Snowmelt-Dominated Headwater Catchments

C. M. Saup[1], S. R. Bryant[1], A. R. Nelson[1], K. D. Harris[1], A. H. Sawyer[1], J. N. Christensen[2], M. M. Tfaily[3,4], K. H. Williams[2,5], and M. J. Wilkins[1,6]

[1] School of Earth Sciences, The Ohio State University, Columbus, OH, USA, [2] Earth Sciences Division, Lawrence Berkeley National Laboratory, Berkeley, CA, USA, [3] Environmental Molecular Sciences Laboratory, Richland, WA, USA, [4] Department of Soil, Water, and Environmental Science, University of Arizona, Tucson, AZ, USA, [5] Rocky Mountain Biological Laboratory, Gothic, CO, USA, [6] Department of Soil and Crop Sciences, Colorado State University, Fort Collins, CO, USA

Correspondence to: M. J. Wilkins, mike.wilkins@colostate.edu

Abstract

Terrestrial and aquatic elemental cycles are tightly linked in upland fluvial networks. Biotic and abiotic mineral weathering, microbially mediated degradation of organic matter, and anthropogenic influences all result in the movement of solutes (e.g., carbon, metals, and nutrients) through these catchments, with implications for downstream water quality. Within the river channel, the region of hyporheic mixing represents a hot spot of microbial activity, exerting significant control over solute cycling. To investigate how snowmelt-driven seasonal changes in river discharge affect microbial community assembly and carbon biogeochemistry, depth-resolved pore water samples were recovered from multiple locations around a representative meander on the East River near Crested Butte, CO, USA. Vertical temperature sensor arrays were also installed in the streambed to enable seepage flux estimates. Snowmelt-driven high river discharge led to an expanding zone of vertical hyporheic mixing and introduced dissolved oxygen into the streambed that stimulated aerobic microbial respiration. These physicochemical processes contributed to microbial communities undergoing homogenizing selection, in contrast to other ecosystems where lower permeability may limit the extent of mixing. Conversely, lower river discharge conditions led to a greater influence of upwelling groundwater within the streambed and a decrease in microbial respiration rates. Associated with these processes, microbial communities throughout the streambed exhibited increasing dissimilarity between each other, suggesting that the earlier onset of snowmelt and longer periods of base flow may lead to changes in the composition (and associated function) of streambed microbiomes, with consequent implications for the processing and export of solutes from upland catchments.

1 Introduction

Upland watersheds play critical roles in biogeochemical cycling of key elements through both the processing and transport of solutes. These

catchments host low-order streams and rivers that are tightly linked to terrestrial elemental cycles (Fasching et al., 2016); within a fluvial network, headwaters receive most of the terrestrial dissolved organic carbon (DOC), which is subsequently stored or processed within highly permeable streambeds (Battin et al., 2008, 2009). The vertical mixing of surface water and groundwater in river and stream beds (termed hyporheic mixing) plays an outsized role in biogeochemical processing in upland catchments (Boano et al., 2014; Gomez-Velez et al., 2014; Gomez-Velez et al., 2015). Vertical mixing results in strong chemical gradients across short physical distances within streambeds. In turn, these physicochemical conditions can support relatively high microbial cell abundances. Estimates suggest that between 10^7 and 10^9, microbial cells are present on every square centimeter of streambed sediment surface. The activity of hyporheic microbiomes results in the processing of organic carbon, the cycling of nitrogen and sulfur species, and changes in the solubility of redox-active metals (Battin et al., 2016; Fasching et al., 2016).

The type and extent of riverbed microbial activity is tightly linked to a range of physicochemical factors, including pore water redox conditions. Greater microbial activity is typically predicted under oxic conditions, while anaerobic, less energetically favorable processes such as sulfate reduction and methanogenesis generally occur under anoxic conditions. In the streambed, redox conditions are at least partly influenced by the extent of hyporheic mixing, which is in turn controlled by hydraulic head gradients between river water and groundwater, as well as the permeability (interconnectedness of pore spaces) of streambed sediments. Under high discharge conditions and the accompanying increase in height of the water column, well-oxygenated river water typically penetrates deep into the streambed, while under base flow conditions and decreased hydraulic head, upwelling anoxic groundwater can displace oxygenated river water. Therefore, changes in the extent, magnitude (i.e., maximum water column height), and timing of snowmelt can directly impact the extent of hyporheic mixing and seasonal patterns of in situ biogeochemical activity (Boano et al., 2014).

A previous investigation into the effects of such seasonal mixing dynamics in the Colorado River near Rifle, CO, revealed that inferred redox fluctuations resulted in a unique “hyporheic microbiome” that was distinct from microbial populations identified in groundwater or surface water chemical end members (Danczak, et al., 2016). Additionally, multiple physicochemical parameters were shown to influence the development of these riverbed microbiomes, resulting in the vertical stratification of microbial communities that significantly differed from each other along a depth gradient (Danczak et al., 2016). These results contrasted with similar studies performed in the Columbia River near Hanford, WA, which indicated that homogenizing selection played a dominant role driving increased similarity between microbial communities in riverbed environments (Graham et al., 2017).

Both the Colorado River at Rifle and the Columbia River at Hanford represent large, high-order rivers. Here we have focused our analyses on an upland catchment (East River) within the Upper Colorado River Basin to understand how seasonally dynamic hydrology affects patterns of hyporheic mixing, pore water biogeochemistry, and microbial community assembly. Such catchments are at the forefront of climate change effects, with changes in vegetation and the timing and extent of snowmelt exacerbated relative to lower elevation locations (de Valpine & Harte, 2001; Elmendorf et al., 2012; Harte & Shaw, 1995; Hubbard et al., 2018; Klein et al., 2004; Panetta et al., 2018; Shaver et al., 2000). Understanding how hydrologic shifts could influence microbiome assembly within the riverbed may be critical for predicting how solutes are processed and transported through these ecosystems under different climate change scenarios.

2 Materials and Methods

2.1 Sample Collection

The three sampling locations in the East River were located before, after, and at the apex of a characteristic meander morphotype along the valley floor. These sampling locations were selected to understand potential variations associated with groundwater discharge and recharge around a prominent meander planform. Each sampling location was located in roughly the middle third of the channel. Using the Geographic Coordinate System, Location A is at 38.923° N, 106.951° W in a riffle area, Location B is at 38.924° N, 106.951° W on the outer edge of a point bar, and Location C is at 38.923° N, 106.951° W along a pool feature (Figure 1). Riffle-pool sequences within the study reach were subtle, and the smaller-scale bedforms such as dunes or scroll bars were not evident in the predominantly gravel substrate. While small-scale bedforms and pool-riffle features all contribute to patterns of surface water-groundwater interaction (Boano et al., 2014), the reach-scale patterns at this site are likely due to a combination of the meander planform and the geologic structure of the subsurface. At each sampling location, temperature data were collected using Onset TMC20-HD temperature sensors deployed at 5, 10, 25, and 35 cm below the sediment-water interface (Bryant et al., 2019). These sensors were manually installed in the streambed and connected to an Onset HOBO 4 Channel External U12-008 Data Logger (Onset Computer Corporation, Bourne, MA, USA) and logged every 15 min over the annual hydrograph. Continuous temperature sensing was complemented with discrete sampling efforts during base flow (August 2016), elevated flow (May 2017), and intermediate flow (late July 2017). Pore water samples were collected at an approximate rate of 5 ml/min using pore water sippers (MHE drive-point groundwater sippers) inserted into the streambed. These samples were collected at a 10-cm resolution over 70-cm vertical profiles. Each sample had a volume of approximately 60 ml. Additionally, sediment grab samples were collected for grain size analysis at all three locations and pooled to form one aggregate sample representative

of the meander. At Location B, a large (~2 L) sample was collected for estimating porosity.

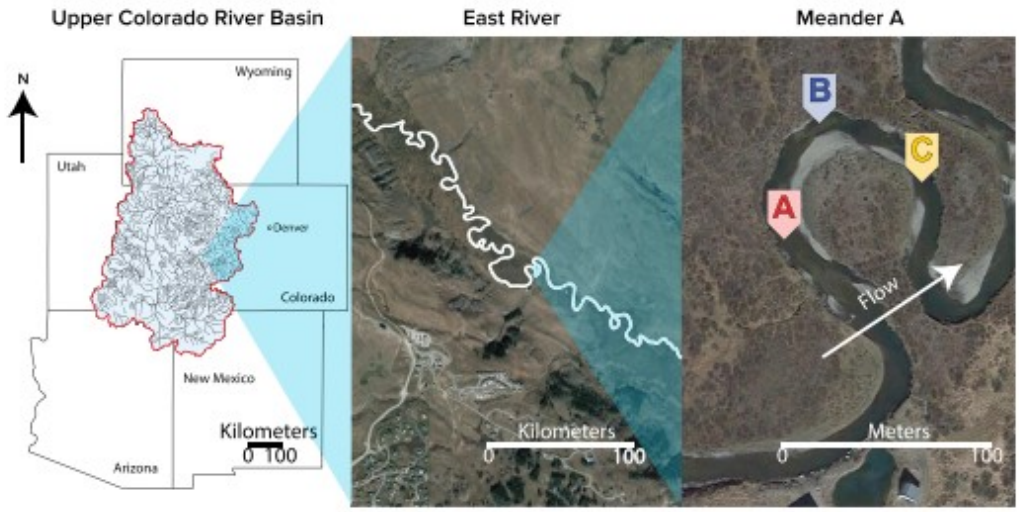

Figure 1. Location of Meander A and Sampling Locations A–C within the East River near Crested Butte, CO, part of the Upper Colorado River Basin.

2.2 Field Analyses

Unfiltered pore water samples from 10-, 20-, and 50-cm depths from each sampling location and season were preserved (refrigerated at 4 °C for 24 hr) for a resazurin-based aerobic respiration assay to track oxygen consumption, which was analyzed using a Horiba Fluoromax 3 spectrofluorometer (Horiba Jobin Yvon Inc. Edison, NJ, USA; Stern et al., 2017). Aerobic respiration measurements were then used to calculate Damköhler numbers to determine the dominance of the oxygen respiration reaction relative to transport processes (Vieweg et al., 2016). Base flow characterization of aerobic respiration was performed in October 2016 instead of August 2016. Following collection, additional fluids were filtered through a 0.22-µm sterivex filter (Fisher Scientific), which was subsequently frozen for later DNA extractions. The resulting filtrate was used in the field for conductivity, redox, pH, and total dissolved solids using a Myron Ultrameter II Model 6PFCE (Myron L Company, Carlsbad, CA, USA). Dissolved oxygen (DO) and sulfide were also quantified in the field using a portable CHEMetrics V-2000 Photometer and Indigo Carmine and Methylene Blue CHEMetrics kits (CHEMetrics, Midland, Virginia).

2.3 Lab-Based Geochemical Analyses

Splits from each pore water sample were filtered in the field through a 0.22-µm filter and immediately placed on ice for analysis of solute chemistry. Acetate, nitrite, nitrate, sulfate, and chloride concentrations in filtrate were measured using an ICS-2100 ion chromatograph equipped with AS-18 analytical and guard columns (Dionex, CA, USA). Total organic carbon, DOC, and dissolved inorganic carbon were measured using a Shimadzu TOC-LCPN

instrument (Shimadzu, MD, USA). Cr, Mn, Fe, Mn, Hg, Mo, Sr, U, Pb, As, Cu, and Zn concentrations were measured at The Ohio State University's Trace Element Research Laboratory using an Inductively-Coupled Plasma Mass Spectrometer. Sr isotopic analyses were performed at Lawrence Berkeley National Laboratory using a chemical separation technique (Christensen et al., 2007; Christensen et al., 2018) to isolate Sr for isotopic analysis on a Triton Multicollector Thermal Ionization Mass Spectrometer (ThermoFisher Scientific, CA, USA). Changes in aqueous carbon pools in the pore fluids were analyzed using a 21 T Fourier Transform Ion Cyclotron Resonance Mass Spectrometer (FTICR-MS) for the presence/absence of all carbon compounds within a sample at the U.S. Department of Energy Environmental Molecular Sciences Laboratory user facility. The spectrometer for the 21 T FTICR-MS consists of a Velos Pro dual linear quadrupole ion trap mass spectrometer (ThermoFisher Scientific, CA, USA) front end that is coupled to a custom FTICR mass spectrometer. Ions were transferred from the Velos Pro to the ICR cell for high-resolution mass analysis by radio frequency-only quadrupole ion guides. ICR signal was acquired using a harmonized ICR cell that utilizes external shimming to approximate an ideal quadrupolar electric field. Samples were directly infused via electrospray ionization at 0.5 ml/min by use of 360-mm outer diameter, 50-mm inner diameter etched fused silica emitters. Before injection, aqueous samples were diluted in methanol (1:2 water:methanol) to improve ionization efficiency. The electrospray voltage was 3.0 kV, and the inlet capillary temperature was 300 °C. Collision-induced dispersion with a 30-V fragmentation energy (Velos Pro) was employed. Mass spectra generated from the average of 400 transient acquisitions by use of an automated gain control target of $3 * 10^6$ for the mass-to-charge ratio (m/z) range 240–1,200 to account for differences in DOC concentrations between the samples. Blanks (high performance liquid chromatography-grade MeOH) were also analyzed at the beginning and the end of the day to monitor potential carry over from one sample to another. All sample peak lists for the entire data set were aligned to each other prior to formula assignment to facilitate consistent peak assignments and eliminate possible mass shifts that would impact formula assignment. Putative chemical formulas were assigned using in-house software “Formularity” (Tolic et al., 2017). Typical mass measurement accuracy was below 50 ppb. Chemical formulas were assigned based on the following criteria: S/N > 7 and mass measurement error <1 ppm, taking into consideration the presence of C, H, O, N, S, and P and excluding other elements. Peaks with m/z values >500 Da often have multiple possible candidate formulas. These peaks were assigned formulas through propagation of CH_2, O, and H_2 homologous series. Additionally, to ensure consistent choice of molecular formula when multiple formula candidates are found the following rules were implemented, we consistently pick the formula with the lowest error, with the lowest number of heteroatoms, and the assignment of one phosphorus atom requires the presence of at least four oxygen atoms. FTICR-MS data were used to characterize bulk shifts in carbon classes using molar H:C and O:C ratios

which can be grouped into different biochemical classes (e.g., lipids, proteins, amino acids, and carbohydrates) using delineations outlined in Kim et al. (2003) and Koch and Dittmar (2006).

2.4 16S rRNA Gene Analyses

16S rRNA genes in extracted DNA were sequenced at Argonne National Laboratory using bacterial/archaeal primer set 515F/806R that targets the V4 region. Resulting reads were checked for chimeras (USEARCH 61 algorithm) and subsequently clustered into exact sequence variant (ESV) classifications at 100% similarities using the DADA2 algorithm in the QIIME2 pipeline (Qiime2-2018.4; (Bolyen et al., 2018) and SILVA 16S rRNA gene database. Subsequent analyses were performed using the R vegan, GUniFrac, and picante packages to determine linkages between geochemical variables and temporal microbial changes. Alpha diversity metrics including Shannon's Diversity Index (H; diversity, vegan package v2.4.4), Faith's Phylogenetic Diversity (PD; pd, picante package v1.6.2), and Pielou's Evenness (J; J = H/log species number) were used to measure the diversity within microbial communities.

Microbial community structure was examined via nonmetric multidimensional scaling (NMDS) ordinations for emergent properties using R v3.3.2 (metaMDS). Both weighted and unweighted UniFrac analyses were also utilized to display changes in microbial community structure through time and space. Vectors overlying the plotted points indicate geochemical parameters and ESVs identified via SIMPER analyses that may drive shifts across microbial communities. Proximity to vectors indicates correlation while vector length indicates magnitude of influence. Significant differences between sampling seasons and locations were determined using global and pairwise permutational analysis of variance (PerMANOVA; Adonis, vegan package v2.4.4) comparisons on UniFrac measurements. 16S rRNA gene sequences obtained in this study are deposited in the NCBI Sequence Read Archive under accession number PRJNA515362.

2.5 Ecological Modeling

To investigate potential ecological drivers within and between seasons, depths, and locations, ecological null modeling was performed following the protocol outlined by Stegen et al. (2013, 2015). Mean nearest taxon distance (MNTD) was calculated for each possible pairwise comparison between samples to capture underlying phylogenetic contributions to community composition. Using 999 community randomizations to create null models, the nearest taxon index (ßNTI) was calculated to determine the deviation of the observed MNTD from the null MNTD. Resulting ßNTI values were used to examine the phylogenetic turnover in each sample, providing insight into whether deterministic (i.e., selection) or stochastic (i.e., random) processes shaped community composition. For example, communities that are more different than would be expected by random chance (ßNTI > 2) occur due to variable selection, which typically results from fluctuating geochemical

conditions. Communities that are more similar than by random chance alone (ßNTI < −2) would occur due to homogenizing selection, which occurs under constant conditions. Finally, if communities are as different as expected by random chance (|ßNTI|< 2), stochastic processes dictate community structure. These stochastic processes can be further distinguished as dispersal limitation (greater than expected turnover; Raup Crick Bray Curtis > 0.95), homogenizing dispersal (less than expected turnover; RCBC < 0.95), and undominated (ecological processes unclear, moderate rate of dispersal and weak selection strength; |RCBC|< 0.95). By combining these metrics, we are able to measure turnover between two communities and identify whether selective (homogenizing/variable) or stochastic (homogenizing dispersal/dispersal limitation) processes dominate (Danczak et al., 2018; Stegen et al., 2013, 2015).

3 Results and Discussion

3.1 Seasonal Hydrology Controls Geochemistry

During the period of study, river discharge (measured using acoustic Doppler velocimetry near the neck of the meander) within the East River was tightly coupled to snowmelt in the watershed, with greatest flow rates occurring in spring and early summer (Carroll & Williams, 2019; Figure 2). Highlighting the linkages between solute concentration dynamics and flow within this system, elevated DOC concentrations were strongly associated with increased river discharge (Figure 2). DOC concentrations in this watershed generally peak slightly before river discharge owing to solute flushing during initial spring snowmelt prior to snowmelt-induced peak discharge and begin to decrease before peak discharge (Winnick et al., 2017). Heat transport models were generated using a one-dimensional heat transfer equation in porous media using observed streambed temperatures. Seepage flux rates revealed a greater influence of upwelling groundwater during periods of low discharge that contrasted with a stronger signal of downwelling river water during periods of snowmelt-driven high river discharge (Figure 2; Bryant et al., 2019). Unfortunately, the high discharge associated with peak flow at Locations B and C damaged temperature probes which could not be safely replaced until discharge decreased. Although broad trends were consistent across the three locations, a stronger groundwater upwelling signal was present at Locations B and C, which resulted in a shorter period of streambed freezing between February and April 2017 (Figure 2).

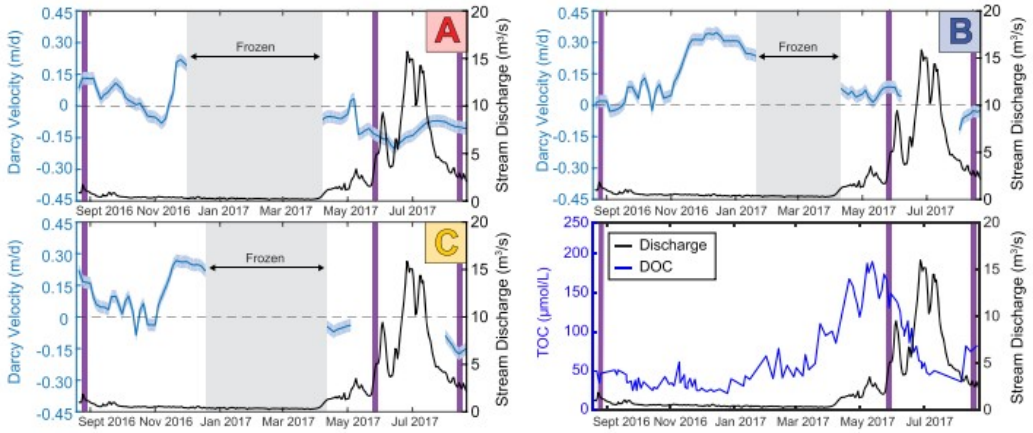

Figure 2. Seepage flux rates as darcy velocity (m/day) for Locations A–C, as well as dissolved organic carbon (DOC) versus stream discharge obtained from Carroll and Williams (2019, fourth panel). Positive darcy velocities represent upwelling, and negative darcy velocities represent downwelling. Purple lines indicate sampling campaigns, and gray boxes indicate periods of streambed freezing.

These in situ measurements were complemented by analysis of strontium isotope ratios in depth-resolved streambed pore fluids, with samples collected during base flow in August 2016, elevated flow in May 2017, and intermediate flow in late July 2017 (Figure 3). The ratio of radiogenic ^{87}Sr relative to stable ^{86}Sr can be used as a tool for age dating materials and tracking fluid migration (Dickin, 1995; Lyons et al., 1995; Palmer & Edmond, 1989; Stewart et al., 1998). Sr isotope results indicated that streambed mixing patterns were highly heterogeneous (uncertainty of $\pm 7 \bullet 10^{-6}$ $^{87}Sr/^{86}Sr$) in the cobble-rich streambed, with Sampling Location B more influenced by a groundwater end-member with a high $^{87}Sr/^{86}Sr$ ratio and Locations A and C more frequently influenced at depth by fluids with lower $^{87}Sr/^{86}Sr$ ratios indicative of river-derived water on longer hyporheic flow paths (Figure 3). These results are consistent with Location B having greater rates of groundwater upwelling over the base flow period and a shorter frozen period in winter.

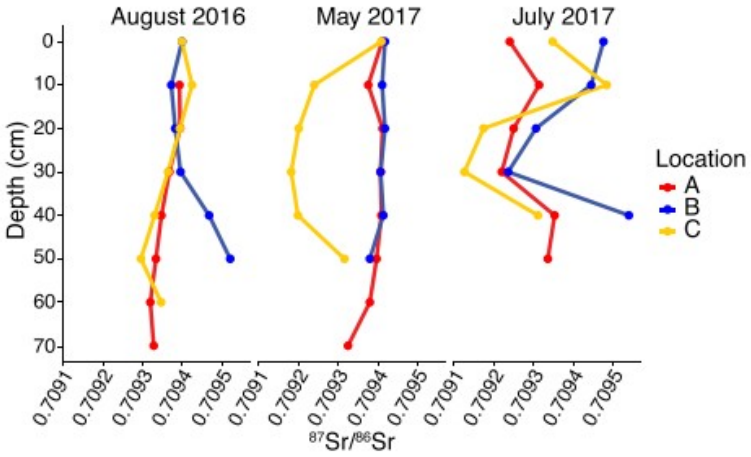

Figure 3. Strontium isotopic composition for each season and location across the 70-cm depth profile.

The analysis of $\delta^{18}O$ and δD in streambed pore fluids further supported inferred mixing patterns. Samples collected under base flow conditions (August 2016) revealed significant isotopic enrichment (−115‰ to −122‰ δD, −15‰ to −17‰ $\delta^{18}O$) relative to isotopically depleted snowmelt-dominated samples collected under high flow conditions in May 2017 (−132‰ to −144‰ δD, −17‰ to −20‰ $\delta^{18}O$), highlighting the importance of evaporative fractionation in this stream system (supporting information Figure S1). This isotopically depleted signal in May 2017 was detected at depth in the streambed, indicating expansion of the zone of hyporheic mixing. Seasonal isotopic trends from May 2017 to July 2017 in surface waters at Locations B and C displayed a more exaggerated change in magnitude than that of their subsurface counterparts, which could be attributed to either buffering from evaporative loss or the influence of isotopically depleted subsurface flow paths (Figure S1).

Downwelling of oxic water during periods of high river discharge should introduce higher concentrations of DO into deeper regions of the streambed, assuming similar consumption rates. Despite clear differences in hyporheic mixing across seasonal time points, depth-resolved DO profiles revealed similar patterns across all sampling events (Figure 4), with DO consistently decreasing with depth into the streambed (Figure 4). The measurement of aerobic respiration rates, via resazurin-based aerobic respiration assay detailed in section 2.2, in the same samples revealed a potential driver behind this observation. As displayed in Figure 4, higher aerobic respiration rates were supported in the streambed during high river discharge and downwelling conditions, relative to measurements performed in August 2016 during base flow. Therefore, greater DO consumption in the streambed under downwelling regimes masks the introduction of DO, resulting in similar profiles through the streambed across seasonal time points. This inference is supported by Peclét and Damköhler calculations >1 for each location and

time point, suggesting that the DO transport-induced oxygen consumption reaction controls porewater concentrations of DO (Saup et al., 2019; equations S1 and S2). Previous work on the lateral distribution of microbial respiration rates also found that DO and nutrient concentrations influence spatial and temporal “hot spots” of biogeochemical activity within the hyporheic zone (King et al., 2014; Reeder et al., 2018). In contrast to the vertical exchange measured here at the East River site, the introduction and rapid depletion of DO along lateral hyporheic flow paths through the floodplain have also been modeled at East River, indicating that complete oxygen consumption occurs over ~1-m distances into the floodplain (Dwivedi et al., 2018).

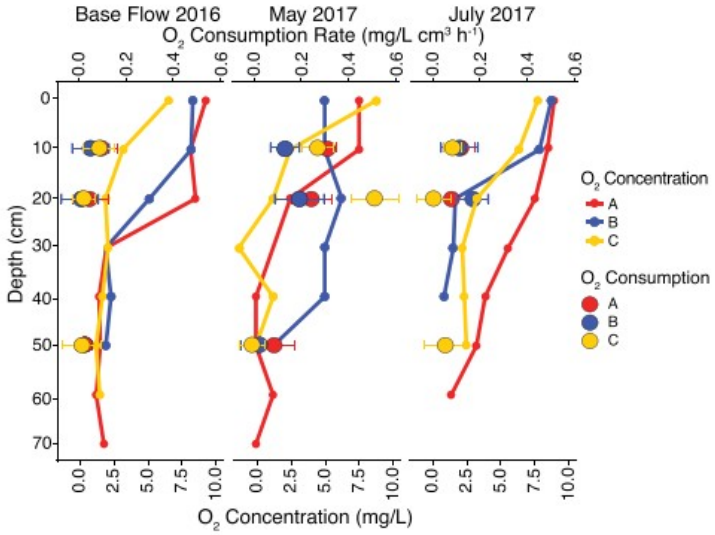

Figure 4. Dissolved oxygen consumption (mg/L • cm^3 • hr^{-1}) measured via resazurin-based aerobic respiration assay and concentration (mg/L) across a 70-cm depth profile at each location. “Base Flow 2016” measurements were collected in October 2016 rather than August 2016 due to infrastructure constraints.

Given the observed seasonal fluctuations in river water DOC concentrations (Figure 2), mass spectrometry tools were applied to both river water and pore water samples to investigate any changes in the composition of the carbon pool. Identified compounds were classified into compositional “pools” based on both their inferred molecular formulae and the nominal oxidation state of carbon (NOSC) in the molecules (Koch & Dittmar, 2006; LaRowe & Van Cappellen, 2011). NOSC values are directly related to the amount of energy required for microbial oxidation of a given compound, with higher NOSC values correlating to lower ΔG_{ox} and therefore a greater energy yield when the reaction is coupled to reduction of a terminal electron acceptor (Boye et al., 2017; LaRowe & Van Cappellen, 2011). On the basis of these classifications, we infer that more diverse carbon substrates with higher NOSC values, albeit at likely lower concentrations, were present in both pore fluids and river water when upwelling conditions were more dominant around the meander (August 2016; Figure 5). These fluids (groundwater and “older”

river water) likely contain organic molecules derived from the underlying Mancos shale and entrained plant DOC, which may explain the diversity of detected compounds. Conversely, although a higher concentration of river water DOC was measured May 2017 during snowmelt-driven elevated flow (Winnick et al., 2017), the carbon pools within these depth-resolved samples were less diverse, with lower NOSC values. While this observation might suggest that DOC derived from the surrounding terrestrial catchment is more compositionally uniform than groundwater carbon pools (Figure 5), the results may also reflect preferential usage and rapid turnover of the energetically favorable, higher NOSC value carbon compounds at a time point where streambed microbial metabolism is the highest (Figure 4; LaRowe & Van Cappellen, 2011).

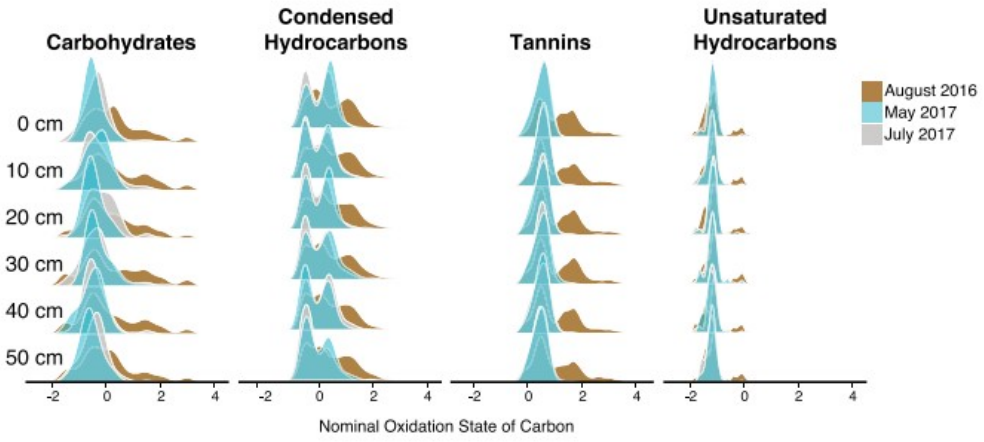

Figure 5. Distribution curves of the nominal oxidation state of carbon for selected carbon classes along a 50-cm depth profile.

3.2 Seasonal Hydrology Controls Microbial Community Dynamics

Microbial communities in the streambed were interrogated using 16S rRNA gene analysis of depth-resolved pore water-sediment slurries. Although no strong depth- or location-dependent trends were observed in any of the alpha diversity metrics, the comparison of samples across seasons revealed differences (Figure S2). Samples collected during base flow (August 2016) were overall less taxonomically and phylogenetically diverse than spring flood (May and July 2017) samples, suggesting that the river water downwelling may act to introduce microorganisms into the streambed and thus drive increases in community diversity. Additionally, the introduction of DO and organic carbon into the streambed from surface water may act to stimulate growth of more diverse microbial assemblages and therefore increase alpha diversity.

ESVs matching a putative metal-reducing phylum, Ignavibacterium, were more abundant with depth and with the onset of base flow (May 2017 < July 2017 < August 2016). Via SIMPER analyses (simper, vegan package v.2.4-2;

Bray & Curtis, 1957), these groups were responsible for approximately 0.05% of the dissimilarity between microbial communities in August 2016 and the other two sampling time points and between 0.5% and 1% of the dissimilarity between microbial communities in shallow samples (0 cm, 10 cm) and deeper samples (40 cm, 50 cm). Microorganisms within this phylum have previously been implicated in diverse anaerobic metabolisms including reduction of oxidized nitrogen species (Liu et al., 2012) and metals (Fortney et al., 2018). Poorly classified members of the Myxococcales displayed similar spatial and temporal trends to Ignavibacteria ESVs, contributing to 1.29% dissimilarity between August 2016 and May 2017 and 1.41% dissimilarity between Sampling Locations A and C. Although taxonomic classification of these ESVs could not be resolved beyond the Order level, *Anaeromyxobacter* species that reside within this group can also utilize a suite of electron acceptors including nitrate and manganese (Sanford et al., 2002).

NMDS and UniFrac ordinations revealed distinct clustering of May 2017 and July 2017 samples away from August 2016 samples (Figure 6). Results from PerMANOVA analyses of the weighted and unweighted UniFrac matrix revealed an overall significant variance across all seasons ($p = 0.035$ and $p = 0.001$, respectively). Pairwise PerMANOVA analyses of the weighted and unweighted UniFrac matrix indicated that while microbial communities detected in August 2016 (base flow) varied significantly with those from May 2017 and July 2017 (higher flow), communities detected in May 2017 and July 2017 did not vary significantly from each other. Although the weighted and unweighted PerMANOVA results show the same trends, it is worth noting that all of the unweighted relationships vary more significantly than all of the weighted relationships (Table S1). Given that unweighted measurements consider only the phylogenetic distance between community members while weighted measurements incorporate both phylogenetic distance and abundance information, these differences could be a result of phylogenetic relationships differing more than relative abundances between seasonal time points, or, less likely, the influence of relic DNA on measured phylogeny (Lennon et al., 2018).

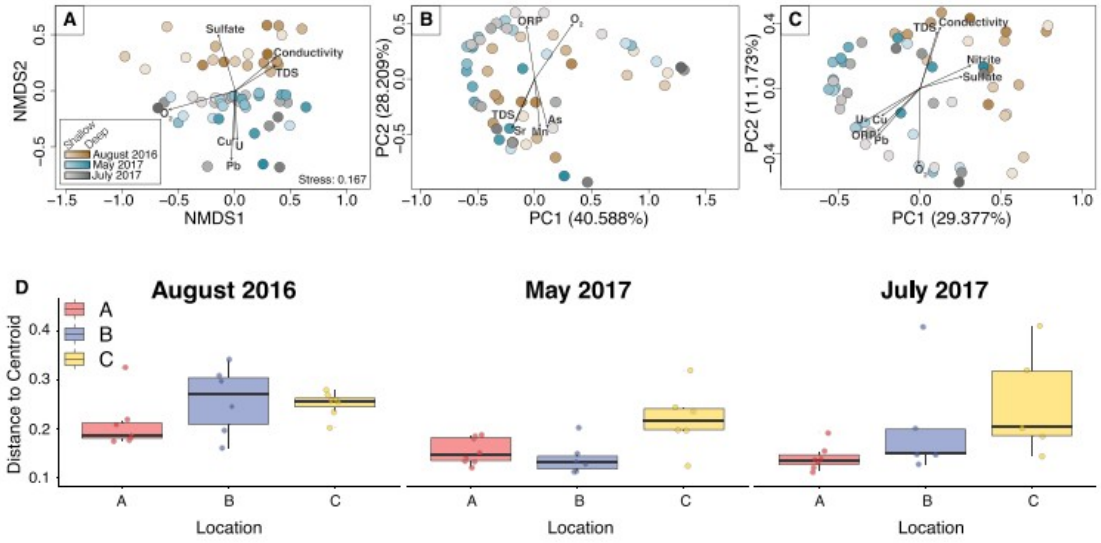

Figure 6. Microbial community beta-diversity measurements parsed by season and depth. (a) Nonmetric multidimensional scaling (NMDS), (b) weighted UniFrac, and (c) unweighted UniFrac. Distances between plotted points of the NMDS are directly linked to their Bray-Curtis dissimilarity. Distances between plotted points of the weighted and unweighted UniFrac analyses are directly linked to their phylogenetic dissimilarity. Vectors indicate geochemical parameters significantly (≤ 0.01) driving the shifts in microbial communities. Proximity to vectors indicates correlation, and vector length indicates magnitude of influence. Color gradient indicates depth. TDS = Total Dissolved Solids; ORP = Oxidation-Reduction Potential. (d) Weighted beta dispersion shown as distance to centroid, parsed by season and location. All locations in May and July 2017 were significantly different than their August 2016 ($p = 0.004$ and 0.01, respectively) counterparts as determined by a permutational analysis of variance analysis.

Chemical measurements collected in May 2017 and applied to the NMDS ordination suggested that DO concentrations may drive differences between shallower samples and deeper samples, reflecting the strong depth-resolved patterns measured in the streambed. Environmental vectors of carbon classes applied to the NMDS and UniFrac ordinations highlighted the relationship between carbon class and seasonal microbial community dynamics with tannins, a plant-derived material flushed into the river during snowmelt, driving differences between higher flow (May and July 2017) and base flow (August 2016) microbial communities. Beta dispersion (“distance to centroid”) calculations performed on the weighted UniFrac ordination also revealed a higher value for samples collected in August 2016 (base flow conditions) relative to spring flood samples collected when there was a greater influence of river water in the bed (Figure 6). This suggests that infiltrating river water may have a “homogenizing” effect throughout the river bed, resulting in microbial communities that are somewhat similar to each other across the depth transect. Conversely, during base flow conditions, upwelling groundwater may drive greater geochemical stratification across the depth profile, resulting in more dissimilar microbial communities.

To further this idea, we investigated how microbial community assembly processes varied across time points and sampling locations. The assembly of

microbial communities is governed by a range of stochastic and deterministic processes including the dispersal of microorganisms, random mutations within the community, and forcings from environmental conditions. Dominant ecological processes acting upon microbial communities can be investigated via null modeling. Briefly, this technique performs pairwise comparisons between measured microbial communities and determines whether any two communities are more similar or more dissimilar than would be expected by random chance. Environmental drivers responsible for these observations can then be applied to the data sets.

These analyses revealed that all the communities, regardless of location or sampling time point, were more similar to each other than would be expected by random chance and were therefore mostly influenced by homogenizing selection (Figure 7). Given the gravel-dominated and hence highly porous and permeable streambed in the East River, we hypothesize that hydrologic mixing leads to homogenization of the communities across a ~50-cm depth transect, as was also inferred from beta dispersion calculations. Furthermore, samples collected in August 2016 under base flow conditions had the least-negative ßNTI values, indicating that these communities were least influenced by homogenizing selection (Figure 7). This observation also tallies with beta dispersion calculations, which suggested that under base flow conditions, streambed microbial communities exhibit a greater degree of dissimilarity. To identify putative geochemical and microbial drivers of shifts in microbial community structure, correlative relationships were determined using a Mantel Test, which revealed significant correlations at every location in August 2016 with conductivity, depth, O_2, Sr, and sulfate. Generally, correlations increased in strength from Location A to Location C (Table S2). Given that hydrologic and geochemical measurements suggest a greater influence of groundwater on the downstream side of the meander (Location C), we infer that the upwelling of geochemically unique groundwater may exert some control over microbial community assembly.

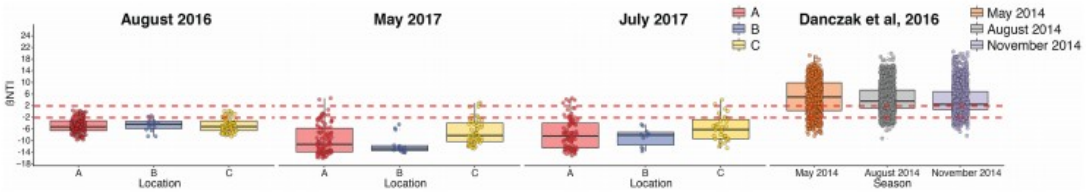

Figure 7. Nearest taxon index (ßNTI) for each location and each season. Seasonal values from Danczak et al. (2016) provided for comparison. Dashed red lines indicate selective pressure delineations; ßNTI > 2 = variable selection; ßNTI < −2 = homogenizing selection; and|ßNTI|< 2 = stochastic process domination.

These results were compared to similar calculations performed on depth-resolved streambed microbial communities in the Colorado River, near Rifle, CO, which is an approximately 1,400-m decrease in elevation from the East River sampling locations. In comparison to the East River, the Rifle sediments

have a similar porosity but much smaller grain size, and permeability is expected to be orders of magnitude lower (Table 1), highlighting the well-characterized relationship between grain size and altitude (McLaren & Bowles, 1985). Reflecting the physical differences between the two systems, depth-resolved communities in the bed of the Colorado River were strongly influenced by variable selection (ßNTI values > 2), indicating that these microbial populations were more dissimilar than would be expected by chance (Figure 7). We hypothesize that physical streambed characteristics, namely, lower permeability, limit the extent to which fluid-entrained microbes can travel, resulting in more spatially constrained communities. Supporting this inference, homogenizing selection was found to play a significant role in microbial community assembly in Columbia River sediments near Hanford, WA (Graham et al., 2017). In contrast to the Colorado River, the sampling location in the Columbia River is characterized by high permeability owing to the Hanford formation underlying the Columbia River (Table 1; Hammond & Lichtner, 2010).

Table 1
Grain Size and Porosity Data for East River and Rifle Streambed Sediments

Sediment Parameters	East River	Colorado River (near Rifle, CO)	Hanford Formation
Porosity (%)	27	30	
D_{50} (mm)	13.26	0.120	
% Mud (<0.063 mm)	1.7	23.9	
% Sand (0.063–2 mm)	11.0	70.6	
% Gravel (> 2 mm)	87.3	5.6	
Permeability (m^2)	10^{-8} to 10^{-5}	10^{-12} to 10^{-8}	10^{-9} to 10^{-8}

Note. Permeability estimates for the East River and the Rifle site are from Freeze and Cherry (1979). Permeability measurements are from Hanford formation sediments bordering the Columbia River (Hammond & Lichtner, 2010).

4 Conclusions

Clear shifts in microbial communities and potential aerobic respiration rates were observed in both the river channel and the streambed associated with hydrologic changes, highlighting the tight linkage between microbial community assembly and seasonal hydrology. Results suggest that aerobic respiration increases with oxygen availability driven by elevated flow during spring snowmelt, potentially stimulating the microbially mediated degradation of more energetically favorable carbon substrates. Microbial diversity metrics reflect these distinct seasonal activity measurements, with well-defined community composition changes driven by spring snowmelt and the onset of base flow. Null modeling revealed homogenizing selection to be the dominant driver of microbial community assembly in the streambed, although periods of base flow (and associated greater influence of upwelling groundwater) were associated with the least negative ßNTI values.

Because of the importance of oxygen as a driver of microbial activity and thus carbon processing in these upland watersheds, it is imperative we understand how this hydrologically dynamic system may be impacted under

future climate change scenarios where decreasing snowpack and earlier onset of snowmelt may result in longer periods of base flow (Adam et al., 2009; Bryant et al., 2013; Christensen & Lettenmaier, 2006; Day & Andrew Day, 2013; Painter et al., 2010, 2018). These changes are predicted to increase net solute export (Dwivedi et al., 2018), with implications for downstream water quality (Hartland et al., 2015; Stucker et al., 2013; Xie et al., 2014). Additionally, increased streambed redox stratification driven by such long-term hydrologic shifts may further replicate the microbially mediated stratification observed here. Whereas vertically resolved communities sampled under base flow were more different from each other (relative to the same profiles under high river discharge), they also exhibited overall lower community diversity with increasing stratification, potentially resulting in changes in ecosystem services provided by the streambed microbial communities. Overall, these data reveal multiple close linkages and feedbacks between physical, chemical, and microbiological processes in headwater streambed ecosystems and highlight the need for increased characterization of upland biogeochemical cycles under future climate change scenarios.

Acknowledgments

We would like to thank the Geological Society of America, the Central Ohio Gem and Mineral Society, and OSU's School of Earth Sciences' Friends of Orton Hall for financial support. This research was supported by the Biological and Environmental Research program in the U.S. DOE Office of Science through Award DE-SC0016488 to M. J. W. and A. H. S. The contributions of J. N. C. and K. H. W. were supported as part of the Watershed Function Scientific Focus Area at Lawrence Berkeley National Laboratory and was supported by the U.S. Department of Energy (DOE) Subsurface Biogeochemical Research Program, DOE Office of Science, Office of Biological and Environmental Research, under Contract DE-AC02-05CH11231. Contributions from M. M. T. were performed using EMSL, a DOE Office of Science User Facility sponsored by the Office of Biological and Environmental Research (BER) and located at Pacific Northwest National Laboratory (PNNL). Special thanks to Robert Danczak for help with statistical tools, Devin Smith for help with isotopic analyses, Anthony Lutton for help with analytical measurements, and Corey Wallace and Michael Whaley for field assistance. Data supporting these conclusions can be found in the ESS-DIVE repository at doi:10.15485/1498798 (Bryant et al., 2019) and doi:10.15485/1504779 (Saup et al., 2019). The authors have no conflicts of interest to disclose.

References

Adam, J. C., Hamlet, A. F., & Lettenmaier, D. P. (2009). Implications of global climate change for snowmelt hydrology in the twenty-first century. *Hydrological Processes*, 23(7), 962– 972.

Battin, T. J., Besemer, K., Bengtsson, M. M., Romani, A. M., & Packmann, A. I. (2016). The ecology and biogeochemistry of stream biofilms. *Nature Reviews. Microbiology*, 14(4), 251– 263.

Battin, T. J., Kaplan, L. A., Findlay, S., Hopkinson, C. S., Marti, E., Packman, A. I., Newbold, J. D., & Sabater, F. (2008). Biophysical controls on organic carbon fluxes in fluvial networks. *Nature Geoscience*, 1(2), 95– 100. https://doi.org/10.1038/ngeo101

Battin, T. J., Kaplan, L. A., Findlay, S., Hopkinson, C. S., Marti, E., Packman, A. I., Newbold, J. D., & Sabater, F. (2009). Erratum: Biophysical controls on organic carbon fluxes in fluvial networks. *Nature Geoscience*, 2(8), 595– 595. https://doi.org/10.1038/ngeo602

Boano, F., Harvey, J. W., Marion, A., Packman, A. I., Revelli, R., Ridolfi, L., & Wörman, A. (2014). Hyporheic flow and transport processes: Mechanisms, models, and biogeochemical implications. *Reviews of Geophysics*, 52, 603– 679. https://doi.org/10.1002/2012RG000417

Bolyen, E., Rideout, J. R., Dillon, M. R., Bokulich, N. A., Abnet, C., Al-Ghalith, G. A., Alexander, H., Alm, E. J., Arumugam, M., Asnicar, F., Bai, Y., Bisanz, J. E., Bittinger, K., Brejnrod, A., Brislawn, C. J., Brown, C. T., Callahan, B. J., Caraballo-Rodríguez, A. M., Chase, J., Cope, E. K., Da Silva, R., Diener, C., Dorrestein, P. C., Douglas, G. M., Durall, D. M., Duvallet, C., Edwardson, C. F., Ernst, M., Estaki, M., Fouquier, J., Gauglitz, J. M., Gibbons, S. M., Gibson, D. L., Gonzalez, A., Gorlick, K., Guo, J., Hillmann, B., Holmes, S., Holste, H., Huttenhower, C., Huttley, G. A., Janssen, S., Jarmusch, A. K., Jiang, L., Kaehler, B. D., Kang, K. B., Keefe, C. R., Keim, P., Kelley, S. T., Knights, D., Koester, I., Kosciolek, T., Kreps, J., Langille, M. G. I., Lee, J., Ley, R., Liu, Y. X., Loftfield, E., Lozupone, C., Maher, M., Marotz, C., Martin, B. D., McDonald, D., McIver, L. J., Melnik, A. V., Metcalf, J. L., Morgan, S. C., Morton, J. T., Naimey, A. T., Navas-Molina, J. A., Nothias, L. F., Orchanian, S. B., Pearson, T., Peoples, S. L., Petras, D., Preuss, M. L., Pruesse, E., Rasmussen, L. B., Rivers, A., Robeson, M. S. 2nd, Rosenthal, P., Segata, N., Shaffer, M., Shiffer, A., Sinha, R., Song, S. J., Spear, J. R., Swafford, A. D., Thompson, L. R., Torres, P. J., Trinh, P., Tripathi, A., Turnbaugh, P. J., Ul-Hasan, S., van der Hooft, J. J. J., Vargas, F., Vázquez-Baeza, Y., Vogtmann, E., von Hippel, M., Walters, W., Wan, Y., Wang, M., Warren, J., Weber, K. C., Williamson, C. H. D., Willis, A. D., Xu, Z. Z., Zaneveld, J. R., Zhang, Y., Zhu, Q., Knight, R., Caporaso, J. G. (2018). QIIME 2: Reproducible, interactive, scalable, and extensible microbiome data science (No. e27295v1). PeerJ Preprints. https://doi.org/10.7287/peerj.preprints.27295v1

Boye, K., Noël, V., Tfaily, M. M., Bone, S. E., Williams, K. H., Bargar, J. R., & Fendorf, S. (2017). Thermodynamically controlled preservation of organic carbon in floodplains. *Nature Geoscience*, 10, 415– 419. https://doi.org/10.1038/NGEO2940

Bray, R. J., & Curtis, J. T. (1957). An ordination of the upland forest communities of southern Winsconin. *Ecological Monographs*, 27, 325– 349. https://doi.org/10.2307/1942268

Bryant, A. C., Painter, T. H., Deems, J. S., & Bender, S. M. (2013). Impact of dust radiative forcing in snow on accuracy of operational runoff prediction in the Upper Colorado River Basin. *Geophysical Research Letters*, 40, 3945– 3949. https://doi.org/10.1002/grl.50773

Bryant, S., Briggs, M., Nelson, A., Saup, C., Wilkins, M., Williams, K., Sawyer, A. (2019): Estimated darcy velocities using temperature time series for meander A of East River, Colorado. Seasonal controls on dynamic hyporheic zone redox biogeochemistry. Ess-dive-6678f7bc54ca137-20190304T232135769. https://doi.org/10.15485/1498798.

Carroll, R., Williams, K. (2019). Discharge data collected within the East River for the Lawrence Berkeley National Laboratory Watershed Function Science Focus Area (water years 2015-2018). Watershed Function SFA. doi:10.21952/WTR/1495380.

Christensen, J. N., Conrad, M. E., DePaolo, D. J., & Dresel, P. E. (2007). Isotopic studies of contaminant transport at the Hanford Site, WA. *Vadose Zone Journal*, 6(4), 1018– 1030. https://doi.org/10.2136/vzj2006.0158

Christensen, J. N., Dafflon, B., Shiel, A. E., Tokunaga, T. K., Wan, J., Faybishenko, B., Dong, W., Williams, K. H., Hobson, C., Brown, S. T., & Hubbard, S. S. (2018). Using strontium isotopes to evaluate the spatial variation of groundwater recharge. *The Science of the Total Environment*, 637, 672– 685.

Christensen, N., & Lettenmaier, D. P. (2006). A multimodel ensemble approach to assessment of climate change impacts on the hydrology and water resources of the Colorado River Basin. *Hydrology and Earth System Sciences Discussions*, 3(6), 3727– 3770.

Danczak, R. E., Johnston, M. D., Kenah, C., Slattery, M., & Wilkins, M. J. (2018). Microbial community cohesion mediates community turnover in unperturbed aquifers. *mSystems*, 3(4). https://doi.org/10.1128/mSystems.00066-18

Danczak, R. E., Sawyer, A. H., Williams, K. H., Stegen, J. C., Hobson, C., & Wilkins, M. J. (2016). Seasonal hyporheic dynamics control coupled microbiology and geochemistry in Colorado River sediments. *Journal of Geophysical Research: Biogeosciences*, 121, 2976– 2987. https://doi.org/10.1002/2016JG003527

Day, C. A., & Andrew Day, C. (2013). Modeling snowmelt runoff response to climate change in the Animas River Basin, Colorado. *Journal of Geology & Geosciences*, 02(01). https://doi.org/10.4172/2329-6755.1000110

de Valpine, P., & Harte, J. (2001). Plant responses to experimental warming in a montane meadow. *Ecology*, 82(3), 637.

Dickin, A. P. (1995). *Radiogenic isotope geology* (452 pp.). Cambridge, UK: Cambridge University Press.

Dwivedi, D., Steefel, C. I., Arora, B., Newcomer, M., Moulton, J. D., Dafflon, B., Faybishenko, B., Fox, P., Nico, P., Spycher, N., Carroll, R., & Williams, K. H. (2018). Geochemical exports to river from the intrameander hyporheic zone under transient hydrologic conditions: East River Mountainous Watershed, Colorado. *Water Resources Research*, 54, 8456– 8477. https://doi.org/10.1029/2018WR023377

Elmendorf, S. C., Henry, G. H. R., Hollister, R. D., Björk, R. G., Bjorkman, A. D., Callaghan, T. V., Collier, L. S., Cooper, E. J., Cornelissen, J. H. C., Day, T. A., Fosaa, A. M., Gould, W. A., Grétarsdóttir, J., Harte, J., Hermanutz, L., Hik, D. S., Hofgaard, A., Jarrad, F., Jónsdóttir, I. S., Keuper, F., Klanderud, K., Klein, J. A., Koh, S., Kudo, G., Lang, S. I., Loewen, V., May, J. L., Mercado, J., Michelsen, A., Molau, U., Myers-Smith, I. H., Oberbauer, S. F., Pieper, S., Post, E., Rixen, C., Robinson, C. H., Schmidt, N. M., Shaver, G. R., Stenström, A., Tolvanen, A., Totland, Ø., Troxler, T., Wahren, C. H., Webber, P. J., Welker, J. M., & Wookey, P. A. (2012). Global assessment of experimental climate warming on tundra vegetation: Heterogeneity over space and time. *Ecology Letters*, 15(2), 164– 175. https://doi.org/10.1111/j.1461-0248.2011.01716.x

Fasching, C., Ulseth, A. J., Schelker, J., Steniczka, G., & Battin, T. J. (2016). Hydrology controls dissolved organic matter export and composition in an Alpine stream and its hyporheic zone. *Limnology and Oceanography*, 61(2), 558– 571. https://doi.org/10.1002/lno.10232

Fortney, N. W., He, S., Kulkarni, A., Friedrich, M. W., Holz, C., Boyd, E. S., & Roden, E. E. (2018). Stable isotope probing for microbial iron reduction in Chocolate Pots Hot Spring, Yellowstone National Park. *Applied and Environmental Microbiology*, 84(11). https://doi.org/10.1128/AEM.02894-17

Freeze, R. A. and Cherry, J. A. (1979). *Groundwater* (Vol. 7632, pp. 604). Englewood Cliffs: Prentice-Hall Inc.

Gomez-Velez, J. D., & Harvey, J. W. (2014). A hydrogeomorphic river network model predicts where and why hyporheic exchange is important in large basins. *Geophysical Research Letters*, 41, 6403– 6412. https://doi.org/10.1002/2014GL061099

Gomez-Velez, J. D., Harvey, J. W., Bayani Cardenas, M., & Kiel, B. (2015). Denitrification in the Mississippi River network controlled by flow through river bedforms. *Nature Geoscience*, 8(12), 941– 945.

Graham, E. B., Crump, A. R., Resch, C. T., Fansler, S., Arntzen, E., Kennedy, D. W., Fredrickson, J. K., & Stegen, J. C. (2017). Deterministic influences exceed dispersal effects on hydrologically-connected microbiomes. *Environmental Microbiology*, 19(4), 1552– 1567. https://doi.org/10.1111/1462-2920.13720

Hammond, G. E., & Lichtner, P. C. (2010). Field-scale model for the natural attenuation of uranium at the Hanford 300 Area using high-performance computing: MODEL FOR NATURAL ATTENUATION OF URANIUM. *Water Resources Research*, 46, W09527. https://doi.org/10.1029/2009WR008819

Harte, J., & Shaw, R. (1995). Shifting dominance within a montane vegetation community: Results of a climate-warming experiment. *Science*, 267(5199), 876– 880. https://doi.org/10.1126/science.267.5199.876

Hartland, A., Larsen, J. R., Andersen, M. S., Baalousha, M., & Ocarroll, D. (2015). Association of arsenic and phosphorus with iron nanoparticles between streams and aquifers: Implications for arsenic mobility. *Environmental Science and Technology*, 49(24), 14,101– 14,109. https://doi.org/10.1021/acs.est.5b03506

Hubbard, S. S., Williams, K. H., Agarwal, D., Banfield, J., Beller, H., Bouskill, N., Brodie, E., Carroll, R., Dafflon, B., Dwivedi, D., Falco, N., Faybishenko, B., Maxwell, R., Nico, P., Steefel, C., Steltzer, H., Tokunaga, T., Tran, P. A., Wainwright, H., & Varadharajan, C. (2018). The East River, Colorado, Watershed: A mountainous community testbed for improving predictive understanding of multiscale hydrological–biogeochemical dynamics. *Vadose Zone Journal*, 17(1). https://doi.org/10.2136/vzj2018.03.0061

Kim, S., Kramer, R. W., & Hatcher, P. G. (2003). Graphical method for analysis of ultrahigh-resolution broadband mass spectra of natural organic matter, the van Krevelen diagram. *Analytical Chemistry*, 75(20), 5336– 5344.

King, S. A., Heffernan, J. B., & Cohen, M. J. (2014). Nutrient flux, uptake, and autotrophic limitation in streams and rivers. *Freshwater Science*, 33(1), 85– 98. https://doi.org/10.1086/674383

Klein, J. A., Harte, J., & Zhao, X.-Q. (2004). Experimental warming causes large and rapid species loss, dampened by simulated grazing, on the Tibetan Plateau. *Ecology Letters*, 7(12), 1170– 1179.

Koch, B. P., & Dittmar, T. (2006). From mass to structure: An aromaticity index for high-resolution mass data of natural organic matter. *Rapid Communications in Mass Spectrometry: RCM*, 20(5), 926– 932.

LaRowe, D. E., & Van Cappellen, P. (2011). Degradation of natural organic matter: A thermodynamic analysis. *Geochimica et Cosmochimica Acta*, 75(8), 2030– 2042.

Lennon, J. T., Muscarella, M. E., Placella, S. A., & Lehmkuhl, B. K. (2018). How, when, and where relic DNA biases estimates of microbial diversity. *MBio*, 9(3), e00637-18.

Liu, Z., Frigaard, N.-U., Vogl, K., Iino, T., Ohkuma, M., Overmann, J., & Bryant, D. A. (2012). Complete genome of Ignavibacterium album, a metabolically versatile, flagellated, facultative anaerobe from the phylum Chlorobi. *Frontiers in Microbiology*, 3, 185.

Lyons, W. B., Tyler, S. W., Gaudette, H. E., & Long, D. T. (1995). The use of strontium isotopes in determining groundwater mixing and brine fingering in a playa spring zone, Lake Tyrrell, Australia. *Journal of Hydrology*, 167(1-4), 225– 239. https://doi.org/10.1016/0022-1694(94)02601-7

McLaren, P., & Bowles, D. (1985). The effects of sediment transport on grain-size distributions. *SEPM Journal of Sedimentary Research*, 55.

Painter, T. H., Deems, J. S., Belnap, J., Hamlet, A. F., Landry, C. C., & Udall, B. (2010). Response of Colorado River runoff to dust radiative forcing in snow. *Proceedings of the National Academy of Sciences of the United States of America*, 107(40), 17,125– 17,130.

Painter, T. H., McKenzie Skiles, S., Deems, J. S., Tyler Brandt, W., & Dozier, J. (2018). Variation in rising limb of Colorado River snowmelt runoff hydrograph controlled by dust radiative forcing in snow. *Geophysical Research Letters*, 45, 797– 808. https://doi.org/10.1002/2017GL075826

Palmer, M. R., & Edmond, J. M. (1989). The strontium isotope budget of the modern ocean. *Earth and Planetary Science Letters*, 92(1), 11– 26. https://doi.org/10.1016/0012-821X(89)90017-4

Panetta, A. M., Stanton, M. L., & Harte, J. (2018). Climate warming drives local extinction: Evidence from observation and experimentation. *Science Advances*, 4(2), eaaq1819.

Reeder, W. J., Quick, A. M., Farrell, T. B., Benner, S. G., Feris, K. P., & Tonina, D. (2018). Spatial and temporal dynamics of dissolved oxygen concentrations and bioactivity in the hyporheic zone. *Water Resources Research*, 54, 2112– 2128. https://doi.org/10.1002/2017WR021388

Sanford, R. A., Cole, J. R., & Tiedje, J. M. (2002). Characterization and description of Anaeromyxobacter dehalogenans gen. nov., sp. nov., an aryl-halorespiring facultative anaerobic myxobacterium. *Applied and Environmental Microbiology*, 68(2), 893– 900.

Saup, C. M., Bryant, S. R., Nelson, A. R., Harris, K. D., Sawyer, A. H., Christensen, J. N., Tfaily, M., Williams, K. H., Wilkins, M. J., (2019). Depth-resolved seasonal porewater chemistry measurements from 3 locations around Meander A of the East River, Colorado. Ess-dive- 4cf9e86a0ad7888-20190325T165401767. doi:10.15485/1504779.

Shaver, G. R., Canadell, J., Chapin, F. S., Gurevitch, J., Harte, J., Henry, G., Ineson, P., Jonasson, S., Melillo, J., Pitelka, L., & Rustad, L. (2000). Global warming and terrestrial ecosystems: A conceptual framework for analysis: Ecosystem responses to global warming will be complex and varied. Ecosystem warming experiments hold great potential for providing insights on ways terrestrial ecosystems will respond to upcoming decades of climate change. Documentation of initial conditions provides the context for understanding and predicting ecosystem responses. *AIBS Bulletin*, 50(10), 871– 882.

Stegen, J. C., Lin, X., Fredrickson, J. K., Chen, X., Kennedy, D. W., Murray, C. J., Rockhold, M. L., & Konopka, A. (2013). Quantifying community assembly processes and identifying features that impose them. *The ISME Journal*, 7(11), 2069– 2079. https://doi.org/10.1038/ismej.2013.93

Stegen, J. C., Lin, X., Fredrickson, J. K., & Konopka, A. E. (2015). Estimating and mapping ecological processes influencing microbial community assembly. *Frontiers in Microbiology*, 6, 370.

Stern, N., Ginder-Vogel, M., Stegen, J. C., Arntzen, E., Kennedy, D. W., Larget, B. R., & Roden, E. E. (2017). Colonization habitat controls biomass, composition, and metabolic activity of attached microbial communities in the Columbia River Hyporheic Corridor. *Applied and Environmental Microbiology*, 83(16). https://doi.org/10.1128/AEM.00260-17

Stewart, B. W., Capo, R. C., & Chadwick, O. A. (1998). Quantitative strontium isotope models for weathering, pedogenesis and biogeochemical cycling. *Geoderma*, 82(1-3), 173– 195. https://doi.org/10.1016/S0016-7061(97)00101-8

Stucker, V. K., Williams, K. H., Robbins, M. J., & Ranville, J. F. (2013). Arsenic geochemistry in a biostimulated aquifer: An aqueous speciation study. *Environmental Toxicology and Chemistry / SETAC*, 32(6), 1216– 1223.

Tolic, N., Liu, Y., Liyu, A., Shen, Y., Tfaily, M., Kujawinski, E. B., Longnecker, K., Kuo, L., Robinson, E., Pasa-Tolic, L., & Hess, N. J. (2017). Formularity: Software for automated formula assignment of natural and other organic matter from ultrahigh-resolution mass spectra. *Analytical Chemistry*, 89(23), 12,659– 12,665.

Vieweg, M., Kurz, M. J., Trauth, N., Fleckenstein, J. H., Musolff, A., & Schmidt, C. (2016). Estimating time-variable aerobic respiration in the streambed by combining electrical conductivity and dissolved oxygen time series. *Journal of Geophysical Research: Biogeosciences*, 121, 2199– 2215. https://doi.org/10.1002/2016JG003345

Winnick, M. J., Carroll, R. W. H., & Williams, K. H. (2017). Snowmelt controls on concentration-discharge relationships and the balance of oxidative and acid-base weathering fluxes in an alpine catchment, East River. *Water Resources Research*, 53, 2507– 2523. https://doi.org/10.1002/2016WR019724

Xie, X., Johnson, T. M., Wang, Y., Lundstrom, C. C., Ellis, A., Wang, X., Duan, M., & Li, J. (2014). Pathways of arsenic from sediments to groundwater in the hyporheic zone: Evidence from an iron isotope study. *Journal of Hydrology*, 511, 509– 517. https://doi.org/10.1016/j.jhydrol.2014.02.006